

## **Distribution Agreement**

In presenting this thesis as a partial fulfillment of the requirements for a degree from Emory University, I hereby grant to Emory University and its agents the non-exclusive license to archive, make accessible, and display my thesis in whole or in part in all forms of media, now or hereafter now, including display on the World Wide Web. I understand that I may select some access restrictions as part of the online submission of this thesis. I retain all ownership rights to the copyright of the thesis. I also retain the right to use in future works (such as articles or books) all or part of this thesis.

Courtney Noetzel

April 1, 2021

Localization of *pezo-1* gene expression responsible for transitioning meiotic to mitotic  
replication in oocytes of *Caenorhabditis elegans*

by

Courtney Noetzel

Steven L'Hernault

Adviser

Biology Department

Steven L'Hernault

Adviser

Guy Benian

Committee Member

William Kelly

Committee Member

2021

Localization of *pezo-1* gene expression responsible for transitioning meiotic to mitotic  
replication in oocytes of *Caenorhabditis elegans*

by

Courtney Noetzel

Steven L'Hernault

Adviser

An abstract of

a thesis submitted to the Faculty of Emory College of Arts and Sciences

of Emory University in partial fulfillment

of the requirements of the degree of

Bachelor of Science with Honors

Biology Department

2021

## Abstract

Localization of *pezo-1* gene expression responsible for transitioning meiotic to mitotic replication in oocytes of *Caenorhabditis elegans*  
By Courtney Noetzel

Fertilization in the nematode *Caenorhabditis elegans* is extraordinarily efficient so that every sperm fertilizes an oocyte entering the wild type hermaphrodite fertilization chamber, the spermatheca. These fertilized oocytes exit the spermatheca, enter the uterus, and transition from meiosis to mitosis as embryogenesis begins. *C. elegans* mutants that affect sperm function, such as *fer-1*, produce defective sperm that are unable to fertilize oocytes. The unfertilized oocytes exit meiosis and become endomitotic because repeated rounds of DNA synthesis occur in the absence of cell division, creating an “Emo” phenotype. A mutant phenotype exists where unfertilized oocytes remain fixed in prophase I of meiosis, creating a “nonEmo” phenotype. The gene responsible for this transition from meiosis to mitosis was identified as *pezo-1*. Tagging the native *pezo-1* gene using CRISPR with mCherry revealed widespread expression of PEZO-1::mCherry including in both the spermatheca and oocytes. Analyzing loss of function mutants revealed which of the 12 alternative splice forms of the wild type *pezo-1* gene are required for wild type (Emo) PEZO-1 function, allowing CRISPR genome engineering to be used to eliminate many irrelevant isoforms. Isoform b, which produces the smallest protein with wild type function, encodes a 2,400 amino acid, predicted to be a 29-pass transmembrane protein that functions as a mechanosensitive ion channel. Looking at PEZO-1::mCherry expression of PEZO-1 isoforms reveals that it retains function and expression across the various isoforms despite large differences in the exons and large intron present. Furthermore, using a chemical agonist that constitutively opens the PEZO-1 ion channel is associated with the nonEmo phenotype. Lastly, using an auxin inducible degradation (AID) system and a GFP targeting nanobody, PEZO-1 is selectively degraded in either the germline or spermatheca, and the associated nonEmo phenotype implies PEZO-1 needs to be expressed in the germline or likely the spermatheca to cause the Emo phenotype. Together, these data give an understanding of how *pezo-1* expression across the isoforms, conformation of the channel, and tissue localization of the protein cause the Emo phenotype. With this understanding, the mechanism of how *pezo-1* expression in the plasma membrane of oocytes causes the Emo phenotype and why the protein evolved may be discovered.

Localization of *pezo-1* gene responsible for transitioning meiotic to mitotic  
replication in oocytes of *Caenorhabditis elegans*

by

Courtney Noetzel

Steven L'Hernault

Adviser

A thesis submitted to the Faculty of Emory College of Arts and Sciences  
of Emory University in partial fulfillment  
of the requirements of the degree of  
Bachelor of Science with Honors

Biology Department

2021

### Acknowledgements

I would like to thank Dr. Steven L'Hernault for allowing me to participate in his lab's research and be a part of this project. His guidance and support allowed me to grow as scientist. I would also like to thank Elizabeth Gleason for being a patient mentor and Huiping Ling for helping with my project. Lastly, thank you to committee members Dr. Guy Benian and Dr. William Kelly for their time and help throughout the process.

## Table of Contents

<b>Chapter 1: Introduction</b>	(1)
<b>Chapter 2: Analysis of PEZO-1 Isoforms Using Fluorescence Microscopy</b>	
A. Introduction	(4)
B. Methods	(5)
C. Results	(6)
D. Discussion	(6)
<b>Chapter 3: Using a PEZO-1 Agonist to Infer the Conformation of PEZO-1 that is Needed to Cause the Emo Phenotype</b>	
A. Introduction	(8)
B. Methods	(8)
C. Results	(9)
D. Discussion	(9)
<b>Chapter 4: Using Auxin Inducible Degradation (AID) System to Infer Tissue Expression of PEZO-1 Required to Produce the Emo Phenotype</b>	
A. Introduction	(11)
B. Methods	(12)
C. Results	(17)
D. Discussion	(19)
<b>Chapter 5: Using a GFP Targeting Nanobody to Infer Tissue Expression of PEZO-1 Required to Produce the Emo Phenotype</b>	
A. Introduction	(21)
B. Methods	(21)
C. Results	(23)
D. Discussion	(23)
<b>Chapter 6: Conclusions and Future Directions</b>	(25)
<b>Figures and Tables</b>	(28)
<b>References</b>	(42)

## Chapter 1: Introduction

*C. elegans* typically exists as a self-fertile hermaphrodite, with two X chromosomes, but rare spontaneous nondisjunction events produce males that have a single X chromosome and can cross-fertilize hermaphrodites (Nigon and Félix, 2017; Zarkower, 2006). The ability of *C. elegans* to maintain a self-fertile population without mating makes them a good model organism for studying fertilization. My project focuses on hermaphrodites because the gene I am studying, *pezo-1* is active during ovulation. As *C. elegans* hermaphrodites mature and undergo gametogenesis, sperm are first produced and then the gonad switches sexual identity and begins oogenesis. The first ovulation pushes the accumulated sperm out of the gonad and into the spermatheca, a contractile chamber where fertilization occurs. (Figure 1; Nishimura and L'Hernault, 2010). Ovulated oocytes are rapidly fertilized as they enter the spermatheca, and this is correlated with oocytes completing meiosis. Fertilized oocytes undergo syngamy, where the haploid oocyte-derived nucleus fuses with the haploid sperm nucleus. The resulting zygote is pushed out of the spermatheca and into the uterus where the mitotic cell divisions of embryogenesis begin to occur (Greenstein, 2005).

In the absence of functional sperm, oocytes cannot be fertilized, yet they still exit meiosis when they enter the spermatheca. However, these unfertilized oocytes do not commence the typical mitotic divisions that lead to a multi-cellular embryo. Rather, unfertilized oocytes undergo continuous endomitotic DNA replication, where the cell becomes polyploidy because cytokinesis never begins. These polyploid nuclei lack distinct, individual chromosomes, which contrasts with the six compact and distinct chromosome pairs that characterize oocytes in diakinesis of meiotic prophase I (Figure 2A; Greenstein, 2005). This continuous endomitotic DNA replication has been named the Emo phenotype (Figure 2B; McCarter et al., 1997). Our lab

has previously found that *pezo-1* is responsible for the switch from meiosis to mitosis and loss of *pezo-1* function causes a nonEmo phenotype where chromosomes in unfertilized, but ovulated, oocytes remain in meiotic prophase I.

PEZO-1 is an inwardly rectifying mechanosensitive ion channel and the only ortholog for the mammalian PIEZO proteins, PIEZO1 and PIEZO2, that exists in *C. elegans* (Bai et al., 2020). PIEZO channels are named for their use of the piezoelectric effect, a phenomenon discovered by Jacques and Pierre Curie, where mechanical stress induces electrical current in highly ordered solid structures with low symmetry (Guerin et al., 2019; Koptsik and Rez, 1981). PIEZO channels have three flexible blade-like structures surrounding the central pore, that function as the force sensors of the protein (Ge et al., 2015). PIEZO proteins were first identified as mechanically gated ion channels in vertebrate hair cells, but the widespread roles they play in mechanotransduction, where mechanical stimuli are translated into biological responses, have since been discovered (Bai, 2020; Corey and Hudspeth, 1979). For example, PIEZO1 has been shown to regulate vascular branching and endothelial cell alignment in humans, and stem cell proliferation in mice models and differentiation in *Drosophila* models (Bai et al., 2018; Del Marmol et al., 2018; He et al., 2018; Li et al., 2015; Nonomura et al., 2018.) PIEZO2 has been shown to regulate light touch, proprioception, and breathing in mice (Bai et al., 2018; Nonomura et al., 2017; Woo et al., 2015; Woo et al., 2015).

Recently, many aspects of PEZO-1 expression in *C. elegans* have been comprehensively characterized, including ovulation and fertilization defects that cause a reduction in brood size of *pezo-1* mutants and the enhancement or suppression of these effects when combined with depletion of cytosolic calcium regulators, sperm signaling and navigation, and tissue specific degradation of PEZO-1 (Bai et al., 2020). While that study of PEZO-1 has been reasonably

thorough, the PEZO-1 protein is responsible for the exit of meiosis in oocytes, and this phenotypic effect of PEZO-1 expression on oocyte replication has been either ignored or not discovered in this past work. When we used CRISPR to tag the native *pezo-1* gene with mCherry, this modified gene exhibits a wild type Emo phenotype, so this phenotypic tag does not detectably affect gene function. We found that *pezo-1::mCherry* expression was widespread, including in both the spermatheca and oocytes (Figure 3). This expression pattern of PEZO-1 leaves unresolved where expression of this protein is required in order to cause the wild type Emo phenotype. My goal in this thesis is to discover if PEZO-1 protein expression is required in the spermatheca, oocyte, or in both of these tissues to cause the Emo phenotype.

## Chapter 2: Analysis of PEZO-1 Isoforms Using Fluorescence Microscopy

### A. Introduction

The large *pezo-1* gene (24.88 Kb) undergoes extensive alternative splicing, giving rise to 12 isoforms of PEZO-1, but why this diversity exists is unknown (Figure 4; Harris et al., 2019). Our lab previously CRISPR engineered *pezo-1::mCherry IV* so as to try to determine the minimal form of *pezo-1* responsible for the Emo phenotype. *pezo-1* Million Mutation alleles (Thompson et al., 2013) were crossed into *fer-1(b232)*, a temperature-sensitive, spermatogenesis-defective mutant allele on chromosome I that causes hermaphrodite self-sterility at 25°C, to allow evaluation of the presence/absence of the nonEmo phenotype (Argon and Ward, 1980). Strain VC20634 *pezo-1(gk364409)* has a stop opal nonsense mutation in the 222<sup>nd</sup> amino acid. The position of this loss of function mutation in exon 5 ruled out splice variants I, J, K, and L as providing wild type PEZO-1 function because they lacked the exon where this mutation was located, yet *fer-1* hermaphrodites still displayed the nonEmo loss of function phenotype when unfertilized oocytes were ovulated (Figure 4). This indicates that isoforms I, J, K, and L are not required for PEZO-1 to cause the normal Emo phenotype. The Emo phenotype was still observed in the absence of exon 8, short and long forms of exon 10 and 14, or the large intron 17. It remains unclear why so many splice variants are necessary if they all produce the Emo phenotype and tissue expression remains the same. Perhaps these alternative forms participate in PEZO-1-regulated processes other than ovulation but, if that is true, such processes are not obvious.

Previously my lab used CRISPR to swap the promoter and 3'UTR of the *pezo-1* gene in attempts to drive its expression exclusively in either the spermatheca or in the oocytes. The native *pezo-1* promoter was swapped for the *jun-1d* promoter, which should drive PEZO-1

expression only in the spermatheca (Hiatt et al., 2009), however we observed mCherry expression in both the spermatheca and the oocytes. The native *pezo-1* 3'UTR was swapped for the *jun-1d* 3'UTR in the strain driven by the *jun-1d* promoter, however the oocytes still had an mCherry signal. The native *pezo-1* promoter was also swapped for the *glh-2* promoter, which should drive PEZO-1 expression only in the oocytes (Spike et al., 2008), however an mCherry signal was still seen in the spermatheca. The native *pezo-1* 3'UTR was swapped for the *pie-1* 3'UTR, which should localize in the germline (Tenenhaus et al., 2001), in the strain driven by the *glh-2* promoter, however an mCherry signal was still seen in the spermatheca. In both *jun-1dpr::pezo-1::jun-1d* 3'UTR and *glh-2pr::pezo-1::pie-1* 3'UTR lines, the large *pezo-1* intron 17 was deleted because we speculated that it might have hidden promoters or enhancers. However, the absence of intron 17 had no obvious effect on mCherry expression, which was still observed in both the soma and the germline. Lastly, the native *pezo-1* 3'UTR was swapped for *unc-54* 3'UTR, which should localize expression in the spermatheca (Merritt et al., 2008), however the oocytes still had an mCherry signal. While the Emo phenotypes were evaluated in many worm strains where PEZO-1 isoforms that were altered by CRISPR engineering, the associated mCherry signal has not been comprehensively examined across all of the PEZO-1 isoforms. These multiple experiments indicate that regulatory sequences that direct cell-specific expression of PEZO-1 reside outside of a typical promoter or 3'UTR sequence.

## B. Methods

I first confirmed that *pezo-1* did not lose its fluorescent signal in specific tissues during CRISPR genome engineering to create the minimal isoform of *fer-1(b232)* I; *pezo-1::mCherry* IV. This involved thawing the various isoform strains that were stored in the -80°C freezer, and raising worms at 16°C until a sufficient number were present. Young worms were then shifted to

25°C, because *fer-1(b232)* causes temperature sensitive sterility due to sperm defects, and mature hermaphrodites were screened for both an mCherry signal and the Emo phenotype. The PEZO-1 isoforms screened include SL1707 *fer-1(b232)* I; *pezo-1::mCherry (ebIs33)* IV (wild type *pezo-1* coding sequence), SL1754 *fer-1(b232)* I; *pezo-1::mCherry (ebIs176)* IV (lacking exon 8 and including long exon 10), SL1753 *fer-1(b232)* I; *pezo-1::mCherry (ebIs175)* I (lacking exon 8 and including short exon 10), SL1765 *fer-1(b232)* I; *pezo-1::mCherry (ebIs62)* IV (lacking exon 8, including short exon 10, and lacking intron 17), SL1776 *fer-1(b232)* I; *pezo-1::mCherry (ebIs71)* (lacking exon 8, including short exon 10, lacking intron 17, and including the long form of exon 14) and SL1777 *fer-1(b232)* I; *pezo-1::mCherry (ebIs72)* IV (lacking exon 8, including short exon 10, lacking intron 17, and including short exon 14; Figure 4).

Worms were placed in 10 µL of 1X M9 buffer solution on poly-L-lysine coated slides. Coverslips were applied to slides that were then placed on a dry ice-chilled metal block in a bucket of dry ice for 5 minutes. After removing the coverslip, the worms were fixed in 4% paraformaldehyde in 1X PBS instead of methanol to preserve the mCherry signal, for 15 minutes. The worms were washed with a PBS + 1% Tween solution three times, using a pulled Pasteur pipette to remove each wash. Then the worms were mounted using 4 µL Invitrogen ProLong Diamond Antifade Mountant with DAPI, left in the dark overnight, and screened for the Emo phenotype and mCherry signal using an Olympus BX60 compound microscope.

### C. Results

As I expected from previous lab results, many of the PEZO-1 isoforms displayed the Emo phenotype. Furthermore, the PEZO-1::mCherry expression remained bright, particularly in the spermatheca and in the plasma membrane of the oocytes across all of the examined PEZO-1 isoforms. Therefore, despite removing exon 8, shortening exons 10 and 14, and removing the

large intron 17, the Emo phenotype and mCherry fluorescent signals remained unaffected, indicating that these parts of the *pezo-1* coding sequence are not required for wild type *pezo-1* function involved in this aspect of ovulation (Figure 5).

#### D. Discussion

My fluorescence microscopy supports the conclusion that the *pezo-1* gene remains competent at producing the Emo phenotype even after extensive coding and potential regulatory sequences are removed by gene editing. Furthermore, the *pezo-1::mCherry* IV isoforms a-f all have a bright fluorescent signal in the spermatheca and the oocytes, meaning that expression patterns remain unchanged and tissue specific alternative splicing is not why the 12 isoforms are present. Isoform b, which encodes a 2,400 amino acid protein, is the minimal form that is able to cause the Emo wild type oocyte phenotype.

Previous work on *C. elegans* PEZO-1 has revealed its widespread role in regulating various aspects of reproduction, particularly ovulation and fertilization, and a number of deletion alleles caused a significant decrease in brood size (Bai et al., 2020). While tissue specific alternative splicing is not the reason for the prevalence of the 12 isoforms, perhaps reproductive capacity varies across the isoforms, allowing some isoforms to have more productive ovulation and fertilization, or increased brood sizes. It also seems possible that there are currently unidentified enhancer sequences that control *pezo-1* expression because previously characterized promoter sequences thought to be tissue-specific in their expression lose this specificity when used to replace the native *pezo-1* promoter, 5' flanking sequence, and 3'UTR.

### **Chapter 3: Using a PEZO-1 Agonist to Infer the Conformation of PEZO-1 that is Needed to Cause the Emo Phenotype**

#### **A. Introduction**

Yoda1 is a small synthetic molecule that binds allosterically and acts as a chemical agonist of mammalian Piezo1, keeping the channel open (Figure 6; Bai et al., 2020; Lacroix et al., 2018). Yoda1 was discovered by screening roughly 3.25 million compounds in a cell-based fluorescence assay and was shown to activate Piezo1 channels in artificial droplet lipid bilayers (Syeda et al., 2015). Yoda1 has been shown to cause a gain of function phenotype in wild type hermaphrodites (Bai et al., 2020), so sterile *fer-1(b232) I; pezo-1::mCherry IV* hermaphrodites were treated with Yoda1 and examined to see if they had an Emo phenotype.

#### **B. Methods**

Adult SL1754 *fer-1(b232) I; pezo-1::mCherry (ebIs175) IV* (lacking exon 8 and including long exon 10) worms were raised at 25°C on Nematode Growth Medium (NGM) agar plates with and without Yoda1. Yoda1 was dissolved in DMSO to create a stock concentration of 10 mM. One mL of this Yoda1 stock solution was added to 500 mL of agar media with NGM for a final concentration of 20 µM Yoda1. The adults were picked off of the plates after they had laid eggs. Once the progeny had become adults, worms were placed in 10 µL of 1X M9 buffer solution on poly-L-lysine coated slides. Coverslips were applied to slides that were then placed on a dry ice-chilled metal block in a bucket of dry ice for 5 minutes. After removing the coverslip, the worms were returned to the frozen metal block and fixed with -20°C methanol for 5 minutes. The worms were washed with a PBS + 1% Tween solution three times, using a pulled Pasteur pipette to remove each wash. Then the worms were mounted using 4 µL Invitrogen

ProLong Diamond Antifade Mountant with DAPI, left in the dark overnight, and screened for the Emo phenotype using an Olympus BX60 compound microscope.

### C. Results

I found that *fer-1(b232)* worms that were not treated with any drugs always have a low level of nonEmo oocytes for some unknown reason (Figure 7). Consequently, I used a one tailed Fisher's exact test to compare the frequency of nonEmo oocytes in Yoda1-exposed and DMSO carrier-only exposed (control) *fer-1* hermaphrodites (Table 1). I found that the p-value ( $\alpha=0.5$ ) indicates that that exposure to Yoda1 causes a significant increase in the observed frequency of the nonEmo phenotype.

### D. Discussion

Yoda1 is a chemical agonist that causes the Piezo1 channel to remain open and my results suggest that this drug causes *fer-1* hermaphrodites with a wild type *pezo-1* gene to exhibit a nonEmo phenotype (Lacroix et al., 2018). My result from this experiment, and the observed nonEmo phenotype in *pezo-1* null mutants, supports the conclusion that the PEZO-1 channel must be closed, or have the gating ability to open and close, in order to produce the Emo phenotype. In other words, the PEZO-1 channel must be closed in order for ovulated oocytes to transition from meiotic arrest to mitotic replication. Alternatively, the nonEmo phenotype resulting from Yoda1 treatment or loss of *pezo-1* function suggests that the level of PEZO-1 activity to achieve the Emo phenotype must be tightly regulated, or the concentration of the ions which pass through the PEZO-1 channel must be at a fairly narrow range. Previous work on PEZO-1 has shown that using Yoda1 in both wild type and *pezo-1* knockout worms will cause a reduction in brood size, meaning that deletion or overactivation of PEZO-1 will result in disrupted brood size (Bai et al., 2020).

The effect of Yoda1 was incomplete in that only 54.2% of the ovulated oocytes in *fer-1* hermaphrodites were nonEmo. One challenge with using pharmacologically-active compounds on *C. elegans* is that this nematode has cuticle that is known to affect permeability of many substances (Xiong et al., 2017). I have tried to double the concentration of Yoda1 to see if this led to further enhancement of the nonEmo phenotype, but this resulted in precipitation of the drug. An alternative way to approach this problem would be to use worms that have altered cuticular permeability, and such mutants, including *bus-5* (Xiong et al., 2017), exist and have been used to address this problem with other drugs; this is further discussed in my Future Directions section (below). However, at this time, it remains an open question as to whether or not this *C. elegans* cuticular permeability issue has affected my results with Yoda1.

## Chapter 4: Using Auxin Inducible Degradation (AID) System to Infer Tissue Expression of PEZO-1 Required to Produce the Emo Phenotype

### A. Introduction

Earlier experimental approaches by me and others explored different ways to try to selectively express *pezo-1* in oocytes or somatic tissues, including the spermatheca. Various strategies using RNAi for either feeding or expression from plasmids using tissue-specific promoters have failed to abolish *pezo-1* expression in a selective manner (E. J. Gleason, unpublished data). WormBase shows that there are no available clones that wholly contain the *pezo-1* gene. Consequently, I have tried to use *in vivo* genetic recombination of two overlapping fosmids that together contained the entire *pezo-1* coding and flanking sequences to reconstruct the intact gene. The strategy we tried to use would have tagged *pezo-1* on its C-terminal end with mCherry, so that the only worms showing the fluorescent red signal would be those with an intact *pezo-1* gene. My plan was to generate an extrachromosomal array and then use genetic mosaic analysis to see the phenotype of worms with *pezo-1* expressed in only oocytes or only the spermatheca, but this plan was not successful because I did not recover the needed, intact *pezo-1* gene. A recently developed technology in *C. elegans* relies on selective degradation of a protein by tissue-specific, ubiquitin-mediated proteolysis (Zhang et al., 2015). I have used this system to further explore if PEZO-1 protein expression is required in either the spermatheca, the oocyte, or in both of these tissues to cause the Emo phenotype. This system uses auxin to induce degradation (AID) of PEZO-1 in either the oocytes or the spermatheca. AID systems allow specific protein degradation by using an adapted *Arabidopsis* TIR1 F-box recognition component of an E3 ubiquitin ligase to deplete degron tagged (in this case, PEZO-1) protein targets in the presence of auxin, a plant hormone involved in cell division, elongation, and differentiation

(Figure 8; Zhang et al., 2015; Teale et al., 2006). We ordered CA1352 *gld-1p::TIR1::mRuby* ::*gld-1 3'UTR* II and CA1200 *eft-3p::TIR1::mRuby* ::*unc-54 3'UTR* II from the *Caenorhabditis* Genetic Center (CGC). Each of these strains includes a TIR1-mRuby F-box gene on chromosome II that is flanked by a promoter and 3' UTR's reported to limit TIR1 expression to either germline (CA1352) or somatic tissue (CA1200) (Zhang et al., 2015). SL1776 *fer-1(b232)* I; *pezo-1::mCherry (ebIs71)* (lacking exon 8, including short exon 10, lacking intron 17, and including the long form of exon 14) contains the shortest form of *pezo-1* currently defined as causing the Emo phenotype (isoform b, see Figure 4). Recent work showed that GFP::PEZO-1, which is fluorescently tagged on the N-terminus, provides wild type PEZO-1 function. Furthermore, *gfp::pezo-1* tagged with a degron at the C-terminal end to produce GFP::PEZO-1::Degron had significant reduction in GFP fluorescence intensities in tissues when TIR1::mRuby expression is induced (Bai et al., 2020). GFP fluorescent intensities were significantly reduced, but the ability of the AID system to completely degrade PEZO-1 in target tissues and its effect on the Emo phenotype remained unknown.

## B. Methods

The sequences acacagcaacaacagaatga and cgcacgattttaaagcggc (IDT; Coraville, IA 52241) were used to place a degron tag at the 5' end of the *pezo-1* gene coding sequence using CRISPR-Cas9 gRNA. We included one additional glycine after the degron sequence to function as a flexible hinge, hopefully allowing PEZO-1 protein folding to not be overly affected by the presence of the degron tag. Alt-R HDR Donor Oligo, containing the degron sequence and two flanking homology arms for accurate double stranded break repair, from IDT was ordered with the sequence

ctgaatcgggtggtcgtaacacagcaacaacagaATGCCTAAAGATCCAGCCAAACCTCCGGCCAAGGC  
 ACAAGTTGTGGGATGGCCACCGGTGAGATCATACCGGAAGAACGTGATGGTTTCCT  
 GCCAAAATCAAGCGGTGGCCCGGAGGCGGCGGCGTTCGTGAAGGGAATGACGGTg  
 CCGCCGCTTTTAAAATCGTG.

Co-CRISPR with *dpy-10* was performed using Alt-R S.p. Cas9 Nuclease V2 from IDT. Dpy and roller worms were screened by PCR using IDT primers EJG174/EJG175 producing a wildtype band of 409 bp and a degon tagged band of 547 bp. The *pezo-1* gene that included the degon encoding sequence was made homozygous, resulting in a genotype of SL1845 *fer-1(b232)* I; *pezo-1(ebIs98 (degon:: pezo-1::mCherry)*IV; *him-5(e1490)* V. Crosses between both of the CA1352 and CA1200 *TIR1::mRuby* strains with SL1845 *ebIs98* were done in order to produce SL1885 *fer-1(b232)* I; *ieSi64(gld-1p::TIR1::mRuby::gld-1 3'UTR)* II; *ebIs98 (degon:: pezo-1::mCherry)* IV for germline TIR1 expression and SL1886 *fer-1(b232)* I; *ieSi57(eft-3p::TIR1::mRuby::unc-54 3'UTR)* II; *ebIs98 (degon::pezo-1::mCherry)* IV for somatic TIR1 expression. When these strains are grown at 25°C to induce sterility and exposed to auxin, PEZO-1 should be degraded in the tissue(s) where the TIR1 F-box protein is expressed. If the nonEmo phenotype is observed, this would identify the tissue(s) where PEZO-1 is required for this trait.

Young F2 worms were placed at 25°C to confirm their *fer-1* I genotype and then screened for a red fluorescent mRuby signal in the germline or somatic tissue for either CA1352 or CA1200 lines and for a red fluorescent mCherry signal in the Olympus SXZ12 dissecting microscope. The two different red signals (mRuby emission= 605 nm; mCherry emission= 610 nm) were impossible to distinguish from each other, so PCR was done on worms with the brightest red signals using primers EJG174/EJG175 to determine if *pezo-1::mCherry* was

present, and if the degron tag was also in the strain. A 409 bp novel DNA insertion would result from a PCR reaction with DNA containing *pezo-1::mCherry*, and a 547 bp novel DNA insertion would result from a PCR reaction with DNA containing *degron::pezo-1::mCherry*. One pedigreed line with the TIR1 transgene that expresses in the germline and one pedigreed line with the TIR1 transgene that expresses in somatic tissues were confirmed to have the expected 547 bp DNA band by agarose gel electrophoresis (data not shown). These two strains were screened for auxin-induced, tissue-specific PEZO-1 degradation.

Adult worms of the two strains were placed on NGM agar plates with and without auxin at 25°C. Adult worms from strains CA1352, CA1200, SL1776, and SL1845 were also placed at 25°C to act as negative controls. The adults were picked off of the plates after they had laid eggs. Once the progeny had become adults, worms were placed in 10 µL of 1X M9 buffer solution on poly-L-lysine coated slides. Coverslips were applied to slides that were then placed on a chilled metal block in a bucket of dry ice for 5 minutes. After removing the coverslip, the worms were returned to the frozen metal block and fixed with -20°C methanol for 5 minutes. The worms were washed with a PBS + 1% Tween solution three times, using a pulled Pasteur pipette to remove each wash. Then the worms were mounted using 4 µL Invitrogen ProLong Diamond Antifade Mountant with DAPI, left in the dark overnight, and screened for the Emo phenotype and mCherry signal using an Olympus BX60 compound microscope.

The mRuby and mCherry signals were impossible to distinguish from one another because they are both red and I could not discern any effect on the PEZO-1::mCherry signal. Consequently, GFP was swapped in to replace the mCherry at the C terminal end of *pezo-1* using CRISPR to yield *fer-1(b232) I*; *TIR1::mRuby II*; *degron::pezo-1::GFP IV*. The goal was to have a green tag on PEZO-1 that was distinct from the red mRuby tag on TIR1 to evaluate the effect

on PEZO-1 removal and to make sure that TIR-1 protein expression was confined to the expected tissue(s). CRISPR-Cas9 gRNA with sequences of *tggaggtggaatggtctcaa* and *actgtcaaatattctgcgaa* were ordered from IDT. Originally, a point mutation from cytosine to guanine was made in a PAM site in the 3' UTR to allow tagging *pezo-1* with mCherry; this point mutation was reverted back to the original cytosine (found in wild type) by the new gBlock containing GFP, a large double stranded DNA fragment containing the sequence for GFP, so that the Cas9 protein does not target the gBlock PAM site. The gBlock ordered from IDT sequence is

GGACACGAATGAGCAAAAAGAAGCAAGAAGCTGGAGGTGGAGGTGGAATGAGTAA  
 AGGAGAAGAATTGTTCACTGGAGTTGTCCCAATCCTCGTCGAGCTCGACGGAGACGT  
 CAACGGACACAAGTTCTCCGTCTCCGGAGAGGGAGAGGGAGACGCCACCTACGGAA  
 AGCTCACCCCTCAAGTTCATCTGCACCACCGGAAAGCTCCCAGTCCCATGGCCAACCC  
 TCGTCACCACCTTCTGCTACGGAGTCCAATGCTTCTCCCGTTACCCAGACCACATGA  
 AGCGTCACGACTTCTTCAAGTCCGCCATGCCAGAGGGATACGTCCAAGAGCGTACC  
 ATCTTCTTCAAaGTcAGcTTAAACATATATATACTAACTACTGATTATTTAAATTTTCA  
 GGACGACGGAAACTACAAGACCCGTGCCGAGGTCAAGTTCGAGGGAGACACCCTCG  
 TCAACCGTATCGAGCTCAAGGTAAGTTTAAACAGTTCGGTACTAACTAACCATACAT  
 AcTTgAAcTTTCAGGGAATCGACTTCAAGGAGGACGGAAACATCCTCGGACACAAGC  
 TCGAGTACAACACTACAACCTCCACAACGTCTACATCATGGCCGACAAGCAAAAAGAAC  
 GGAATCAAGGTCAACTTCAAGGTAAGTTTAAACATGATTTTACTAACTAACTAagatttaa  
 atatttcactgtcaaatattctgcgaaccgaaccatcgtaatacattttatttttactttctctgtttctc.

Co-CRISPR with *dpy-10* II was performed using Alt-R S.p. Cas9 Nuclease V3 from IDT. *Dpy* and roller worms were screened by PCR using IDT primers EJG428F/EJG430R. A 1125 bp insertion results from a PCR reaction containing mCherry, an 890 bp insertion results from a

PCR reaction containing GFP. The GFP line was crossed in and made homozygous to yield *degron::pezo-1::GFP* IV in one line that also had *TIR1::mRuby* expressed in the germline and one line that also had *TIR1::mRuby* expressed in the somatic tissue.

Adult worms were placed on NGM agar plates with and without auxin at 25°C. The adults were picked off of the plates after they had laid eggs. Once the progeny had become adults, worms were placed in 10 µL of 1X M9 buffer solution on poly-L-lysine coated slides. Coverslips were applied to slides that were then placed on a dry ice-chilled metal block in a bucket of dry ice for 5 minutes. After removing the coverslip, the worms were returned to the frozen metal block and fixed with -20°C methanol for 5 minutes. The worms were washed with a PBS + 1% Tween solution three times, using a pulled Pasteur pipette to remove each wash. Then the worms were mounted using 4 µL Invitrogen ProLong Diamond Antifade Mountant with DAPI, left in the dark overnight, and screened for the Emo phenotype and GFP signal using an Olympus BX60 compound microscope.

The CRISPR C terminal tagged GFP fluorescent signal was not bright enough to see in live or fixed worms unlike the mCherry tag, so immunofluorescence using antibodies to GFP was done in addition to the PCR to confirm that the GFP was present in *fer-1(b232)* I; *TIR1::mRuby* II; *degron::pezo-1::GFP* IV worms. Worms were placed in 8 µL Sperm Medium dissection solution [40 µL 5X Sperm Medium stock solution (250 mM HEPES pH7.8, 125 mM KCl, 225 mM NaCl, 5 mM MgSO<sub>4</sub>, 25 mM CaCl<sub>2</sub>), 1.8 µL 20% dextrose, 158.2 µL H<sub>2</sub>O] on a poly-L-lysine coated slide. The immunofluorescence worked best when the gonads of the worms were exposed, so worms were dissected at the vulva with a 27-gauge needle to release the gonads. Coverslips were applied to slides that were then placed on a dry ice-chilled metal block in a bucket of dry ice. After removing the cover slip, the slides were placed in a Coplin jar filled

with -20°C methanol. The methanol-filled Coplin jar with slides was put in the freezer at -20°C for 15 minutes. The worms were rehydrated slowly by adding 20% more PBS Tween (PBS + 1% Tween) to the Coplin jar and waiting two minutes. 50% of the solution was poured out, the Coplin jar was filled back up with PBS Tween, and the slides in the Coplin jar were incubated for two minutes. This wash step was repeated three times, and then the slides were washed an additional three times, pouring out all the PBS Tween each time. The slides were then permeated for five minutes using 0.2% Triton X-100 in PBS Tween in a Coplin jar. The slides were then washed three times with PBS Tween. 50 µL of Block (800 µL 1X PBS Tween + 200 µL Normal Donkey Serum + 0.02 g BSA) was placed on the worms, and the slides were left to incubate in a humid chamber for 60 minutes. The block solution was aspirated off with a pulled Pasteur pipette, and 50 µL of primary antibody (Aves Chicken anti GFP at 1:1000 in block) was added. The slides were left in a humid chamber at room temperature for two hours and then placed at 4°C overnight. The slides were then washed four times with 1X PBS Tween in a Coplin jar and left to rest for 10 minutes in the dark. 100 µL of secondary antibody (1:2000 Jackson ImmunoResearch Donkey anti-Chicken IgY (H+L), in 20% block and 1X PBS Tween) was added to the slides and left to incubate for one hour at room temperature. The slides were washed three times with 1X PBS Tween in a Coplin jar and two times with PBS. Then the worms were mounted using 4 µL Invitrogen ProLong Diamond Antifade Mountant with DAPI, left in the dark overnight, and screened for the Emo phenotype using an Olympus BX60 compound microscope.

### C. Results

In both the SL1885 *fer-1(b232)* I; *ieSi64(gld-1p::TIR1::mRuby::gld-1 3'UTR)* II; *ebIs98 (degron::pezo-1::mCh)* IV and SL1886 *fer-1(b232)* I; *ieSi57(eft-3p::TIR1::mRuby::unc-54*

3'UTR) II; *ebIs98 (degron::pezo-1::mCherry)* IV an increase in the nonEmo phenotype was seen when worms were exposed to auxin. A one tailed Fisher's exact test was used to compare whether or not auxin exposure caused a significant elevation in the frequency of observing the nonEmo phenotype in *fer-1(b232)* I; *TIR1::mRuby* II; *degron::pezo-1::mCherry* IV (Table 2). The calculated p-values ( $\alpha=0.5$ ) showed that the observed elevation in the frequency of the nonEmo phenotype after exposure to auxin was significant.

The strain CA1200 expresses a TIR1::mRuby F-box protein that was supposed to be expressed specifically in somatic tissue, but I observed that the distal gonads of this strain had an mRuby nuclear signal in oocytes similar to that of CA1352, which was supposed to be limited in its expression of the TIR1::mRuby F-box protein to the germline (Bai et al., 2020; Figure 9).

The red mRuby and mCherry signals were impossible to distinguish from one another, so I could not determine if PEZO-1 was being degraded in *fer-1(b232)* I; *TIR1::mRuby* II; *degron::pezo-1::mCherry* IV worms (Figure 10). Consequently, GFP was swapped in to replace mCherry resulting in the genotype *fer-1(b232)* I; *TIR1::mRuby* II; *degron::pezo-1::GFP* IV. Unlike PEZO-1::mCherry, the PEZO-1::GFP signal was not visible in the Olympus BX60 compound microscope, so I performed both immunofluorescence and PCR to conform that GFP was present in these strains. The immunofluorescence worked best when the gonads were dissected out of the hermaphrodites, and I observed a GFP signal in the plasma membrane of the oocytes (Figure 10).

In *fer-1(b232)* I; *TIR1::mRuby* II; *degron::pezo-1::GFP* IV worms expressing TIR1::mRuby in the germline or somatic tissues, auxin exposure was correlated with an increase in the nonEmo phenotype. A one tailed Fisher's exact test was used to compare the significance of auxin exposure on the nonEmo phenotype in *fer-1(b232)* I; *TIR1::mRuby* II; *degron::pezo-*

*I::GFP* IV worms (Table 2). The calculated p-values ( $\alpha=0.5$ ) showed that the observed elevation in the frequency of the nonEmo phenotype after exposure to auxin was significant.

#### D. Discussion

My results suggest that degradation of PEZO-1 in either the germline or somatic tissue is sufficient to cause a significant increase in the nonEmo phenotype, meaning PEZO-1 needs to be expressed in either the germline or somatic tissue for oocytes to transition from meiosis to mitosis. However, the mRuby signal overlapped that of the *degron::PEZO-1::mCherry* signal and distinguishing these two red signals proved to be impossible. Prior work claimed that *pezo-1* tagged with GFP on the N terminal end had bright expression in the spermatheca and in the membrane of oocytes (Bai et al., 2020). In contrast, the CRISPR C terminal tagged GFP fluorescent signal in my experiments was not bright enough to see in live or fixed worms unlike prior work (Bai et al., 2020) or my other work with mCherry tagged PEZO-1. So, I was unable to directly observe the degradation of *degron::PEZO-1::GFP*. Although both PCR and immunofluorescence confirmed that GFP was present in the strains I characterized, it remains unclear why the GFP signal was not bright enough to be observed in live animals.

There was expression of *TIR1::mRuby* in the nucleus of the oocytes in the distal gonad of the lines that should only be expressing TIR1 in somatic tissue, making it difficult to draw a definitive conclusion about the phenotypic effects of somatic PEZO-1 degradation. It is possible that PEZO-1 is being degraded in both the somatic tissue(s) and the germline. Also, my result for PEZO-1 degradation in the germline upon exposure to auxin was stronger than my result for PEZO-1 degradation in the somatic tissues, suggesting that PEZO-1 expression in the germline is more important for causing the Emo phenotype. However, it is possible the *gld-1* promoter may be stronger than the *eft-3* promoter, which would result in greater TIR1 activity in lines

expressing TIR1 in the germline than in lines expressing TIR1 in the somatic tissue. Both of these results suggest it is likely that PEZO-1 needs to be expressed in the germline to produce the Emo phenotype, but whether PEZO-1 expressed in the spermatheca can produce the Emo phenotype is still unclear.

## Chapter 5: Using a GFP Targeting Nanobody to Infer Tissue Expression of PEZO-1 Required to Produce the Emo Phenotype

### A. Introduction

*TIR1::mRuby* II was found to be expressed in the nucleus of the oocytes in the distal gonad, in both *gld-1p::TIR1::mRuby::gld-1 3'UTR* II where it should be expressed and *eft-3p::TIR1::mRuby::unc-54 3'UTR* II, which are published as specifically expressing *TIR1::mRuby* II in the germline and somatic tissue respectively (Zhang et al., 2015). Furthermore, both germline and somatic *TIR1::mRuby* II showed an increase in the nonEmo phenotype in *fer-1(b232)* I; *TIR1::mRuby* II; *degron::pezo-1::mCherry* IV and *fer-1(b232)* I; *TIR1::mRuby* II; *degron::pezo-1::GFP* IV when raised at 25°C, however the expressivity was not complete. To independently confirm the result of somatic *TIR1::mRuby* II degrading *degron::PEZO-1::mCherry* to cause the nonEmo phenotype, line MLC1092 *lucSi100* II (*hsp16.14::vhhGFP::zif-1::SL2::mCherry::his-11::tbb2 3'UTR*); *unc-119* III, containing a nanobody that has been shown to target GFP-tagged proteins for degradation using a ZIF-1 recognition component known to function only in somatic tissue under the control of a heat shock promoter was used (Charest et al., 2020).

### B. Methods

Strain MLC1094 *lucSi100* (*hsp16.41::vhhGFP4::zif-1::SL2::mCherry::his-11::tbb-2 3'UTR*) II; *unc-119* III was ordered from *Caenorhabditis* Genetic Center (CGC) (Charest et al., 2020). *LucSi100* II; *unc-119* III was crossed with *fer-1(b232)* I; *TIR1::mRuby* II; *degron::pezo-1::mCherry* IV; *him-5 V* to yield *fer-1 (b232)* I; *lucSi100::mCherry* II; *degron::pezo-1::mCherry* IV; *him-5 V*. F1 progeny were screened for males, confirming the cross worked and *him-5 V* was present. F1 hermaphrodites from successful mates were picked to their own plate to

self-fertilize. F2 progeny were shifted up to 25°C to check for *fer-1(b232)* I and a *lucSi100* II mCherry signal in the Olympus SXZ12 dissecting microscope. This strain was crossed with *fer-1(b232)* I; *dpy-10::TIR1::mRuby* II; *degron::pezo-1::GFP* IV and made homozygous to yield *fer-1(b232)* I; *lucSi100::mCherry* II; *degron::pezo-1::GFP* IV. Parent worms were screened for GFP in a PCR reaction with primers EJG428F/EJG430R. A 1125 bp insertion results from a PCR reaction containing mCherry, an 890 bp insertion results from a PCR reaction containing GFP, and a 246 bp fragment results from a wild type PCR. Progeny were shifted up to 25°C to check for *fer-1(b232)* I and *lucSi100* II mCherry signal in the Olympus SXZ12 dissecting microscope. Worms were raised at 25°C and then heat shocked for 30 minutes at 30°C to induce the heat shock promoter, *vhhGFP4::zif-1*, to degrade *pezo-1::GFP* IV. Worms were heat shocked for 30 minutes and left at 25°C for both two hours and seven hours. Furthermore, line *fer-1(b232)* I; *lucSi100::mCherry* II *degron::pezo-1::GFP* IV worms that were raised at 25°C and not heat shocked, line *fer-1(b232)* I; *lucSi100::mCherry* II without GFP and with the heat shock system, and line and *fer-1(b232)* I; *TIR1::mRuby* II; *degron::pezo-1::GFP* IV with GFP and without the heat shock system were used as controls.

Worms heat shocked for 30 minutes and left at 25°C for two hours and seven hours, and control worms, were placed in 10 µL of 1X M9 buffer solution on poly-L-lysine coated slides. Coverslips were applied to slides that were then placed on a dry ice-chilled metal block in a bucket of dry ice for 5 minutes. After removing the coverslip, the worms were returned to the frozen metal block and fixed with -20°C methanol for 5 minutes. The worms were washed with a PBS + 1% Tween solution three times, using a pulled Pasteur pipette to remove each wash. Then the worms were mounted using 4 µL Invitrogen ProLong Diamond Antifade Mountant with

DAPI, left in the dark overnight, and screened for the Emo phenotype and GFP signal using an Olympus BX60 compound microscope.

### C. Results

Worms that were heat shocked for 30 minutes at 30°C were almost completely nonEmo. Furthermore, *fer-1(b232) I; lucSi100 II (hsp16.14::vhhGFP::zif-1::sl2::mCherry::his-11::tbb2 3'UTR); pezo-1::GFP IV* control worms that were not heat shocked at 30°C also showed an elevated frequency of the nonEmo phenotype. A one tailed Fisher's test was used to compare the significance between each of the control groups and each of the *fer-1(b232) I; lucSi100 II (hsp16.14::vhhGFP::zif-1::sl2::mCherry::his-11::tbb2 3'UTR); pezo-1::GFP IV* heat shocked experimental groups. The control group that was not heat shocked but had the heat shock system was also tested for significance against the other two control groups. The p-values ( $\alpha=0.5$ ), indicate that the percentage of nonEmo phenotype observed in worms with the heat shock promoter system as compared to controls is significant (Figure 11, Table 3).

### D. Discussion

My results imply that degradation of PEZO-1 in somatic tissue by the GFP targeting nanobody is sufficient to cause the nonEmo phenotype, meaning that PEZO-1 expressed in somatic tissue causes the transition from meiosis to mitosis in oocytes. There was a significant increase in *fer-1(b232) I; lucSi100 II (hsp16.14::vhhGFP::zif-1::sl2::mCherry::his-11::tbb2 3'UTR); pezo-1::GFP IV* control worms that were not heat shocked at 30°C in comparison to the other control groups, therefore it is likely that the heat shock promoter *hsp16.14*, has some activity at 25°C.

My data with this experiment independently supports my data from the AID experiment, confirming that PEZO-1 expression in the spermatheca results in the Emo phenotype. It is

possible however, that the anti-GFP nanobody ZIF-1 complex is also targeting PEZO-1::GFP in the germline. Based on these data, it is likely that PEZO-1 expressed in the spermatheca causes the Emo phenotype, but it is not certain. Protein expression in both tissues being sufficient to cause the Emo phenotype would result in two different mechanisms that are responsible for the switch from meiosis to mitosis. While possible, this would result in a more complex evolutionary history of the PEZO-1 protein's role in reproduction.

## Chapter 6: Conclusions and Future Directions

Fluorescence microscopy revealed that the Emo phenotype is unaffected and there is not tissue specific expression for PEZO-1 across the alternative splice variants, making their reason for existence unclear. Future experiments should further edit the *pezo-1* gene using CRISPR on the minimal form, isoform b, to discover which specific sequence is necessary for the Emo phenotype. However, in doing so, off target effects such as decreased brood size, and ovulation and sperm navigation defects may be observed, making it difficult to identify the minimal form (Bai et al., 2020). In addition, other promoters and 3' UTRs should be explored in order to achieve tissue specific expression of the *pezo-1::mCherry* IV. In particular, a spermathecal specific promoter, *fln-1* should be swapped out for the native the *pezo-1::mCherry* IV promoter to determine if it will drive expression of PEZO-1::mCherry in the spermatheca as claimed in published work (Kovacevic et al., 2013).

Determining the tissues where PEZO-1 is required is important because this protein controls the transition from meiotic to mitotic cell division in oocytes. This will also provide insight into the mechanism of how PEZO-1 activity is able to mediate the endomitotic DNA replication that happens when oocytes are ovulated but not fertilized. My Yoda1 experiment showed that the PEZO-1 ion channel needs to either be closed, or have the gating ability to open and close, in order to produce the wild type Emo phenotype. PEZO-1 has been shown to be an inwardly rectifying ion channel, showing a preference for calcium, therefore with the Yoda1 experiment revealing the closed conformation causes the Emo phenotype, it is possible that a buildup of calcium in the extracellular matrix is necessary for the transition to mitosis (Bai et al., 2020). This is consistent with the nonEmo phenotype arising from treatment with Yoda1 agonist and deficiency of PEZO-1 in a *pezo-1* mutant.

Sterile *fer-1(b232)* I; *bus-5(br19)* X should also be examined for sensitivity to Yoda1 because *bus-5(br19)* mutants have a cuticle that is more permeable in comparison to wild type worms, potentially allowing this drug to function at a lower working concentration with, perhaps, more penetrant effect on the Emo phenotype (Xiong et al., 2017). DC19 *bus-5(br19)* X hermaphrodites will be mated with permissively raised SL154 *fer-1(b232)* I; *him-5(e1490)* V males and transferred to new plates each day (Xiong H et al., 2017). F1 progeny will be screened for males to ensure that the cross was successful, and hermaphrodite F1s will be picked to their own plate to self-fertilize. F2 worms that exhibit slow movement and wide tracks, indicating the presence of *bus-5* will be picked to their own plate, and the progeny of the F2 worms will be shifted up to 25°C to induce sterility and check to see if the worms are homozygous for *fer-1*. The F3 worms will be checked again by PCR and restriction digest with primers *bus-5F/bus-5R* to confirm they are homozygous for *bus-5*, giving rise to *fer-1(b232)* I; *him-5(e1490)* V; *bus-5(br19)* X. Adult worms will be grown on NGM agar plates with and without Yoda1, and their progeny will be DAPI stained and screened for the nonEmo phenotype.

My results from the auxin inducible degradation (AID) experiment support the conclusion that PEZO-1 expressed in either the germline or spermatheca is sufficient to produce an Emo phenotype. There was significant increase of the nonEmo phenotype when comparing worms exposed to auxin to those not exposed to auxin in the expression of TIR1::mRuby in both the germline and somatic tissue. This implies that PEZO-1 expressed in either the germline or somatic tissue is sufficient to cause the Emo phenotype, however, the similar expression in the germline of strains that were supposed to express TIR1::mCherry in somatic tissue raises the possibility that TIR1::mCherry has leaky expression, and PEZO-1 was degraded in both tissues. This confirms that PEZO-1 likely needs to be expressed in the germline, but it is still unclear if

PEZO-1 expressed in the spermatheca will cause the Emo phenotype. However, whether PEZO-1 is expressed in the germline only or in the germline and spermatheca to cause the Emo phenotype, both instances would result in a buildup of calcium in the extracellular matrix. PEZO-1 being expressed in both tissues may have a greater buildup.

The GFP targeting nanobody experiment allowed degradation of PEZO-1::GFP in somatic tissue, and resulted in a significant increase in the nonEmo phenotype. This confirmed that PEZO-1 expressed in somatic tissue is sufficient to cause the Emo phenotype with an independent experiment. One potential problem with this experiment was that I could not directly observe the effect on PEZO-1::GFP in living animals. This means that there is a possibility that the GFP targeting nanobody was not limited to somatic tissue and PEZO-1 expressed in the germline was also targeted for destruction, resulting in the nonEmo phenotype.

While the data from the AID system experiment and the GFP targeting nanobody experiment together imply that that PEZO-1 can be expressed in the germline or somatic tissue to cause the Emo phenotype, PEZO-1 expression in two locations to cause a change in DNA replication within oocytes is not a parsimonious explanation. Future experiments should further explore PEZO-1 expression in the spermatheca and the associated phenotype and might include using CRISPR to identify a spermathecal tissue specific isoform, using CRISPR to engineer a line with a spermathecal specific promoter and 3'UTR, or exploring other degradation systems that specifically target the spermatheca.

## Figures and Tables

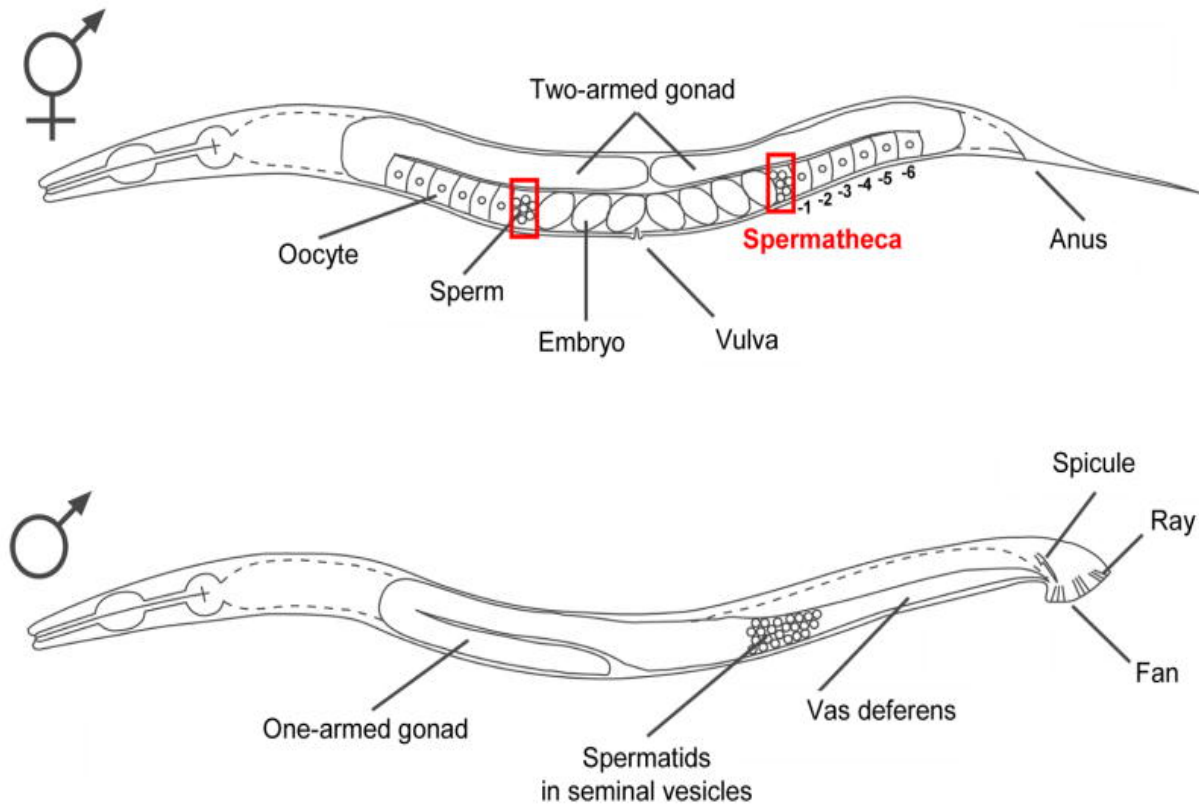


**Figure 1.** Hermaphrodite and male reproductive system of *C. elegans* (Nishimura and L'Hernault, 2010). The top picture displays the reproductive structures of a hermaphrodite worm. Mature oocytes are fertilized by sperm in the spermatheca, highlighted in red. Once fertilized, mature zygotes exit the worm into the external environment through the vulva. The bottom picture shows a male, which were used for genetic crosses but otherwise, not characterized in my thesis.

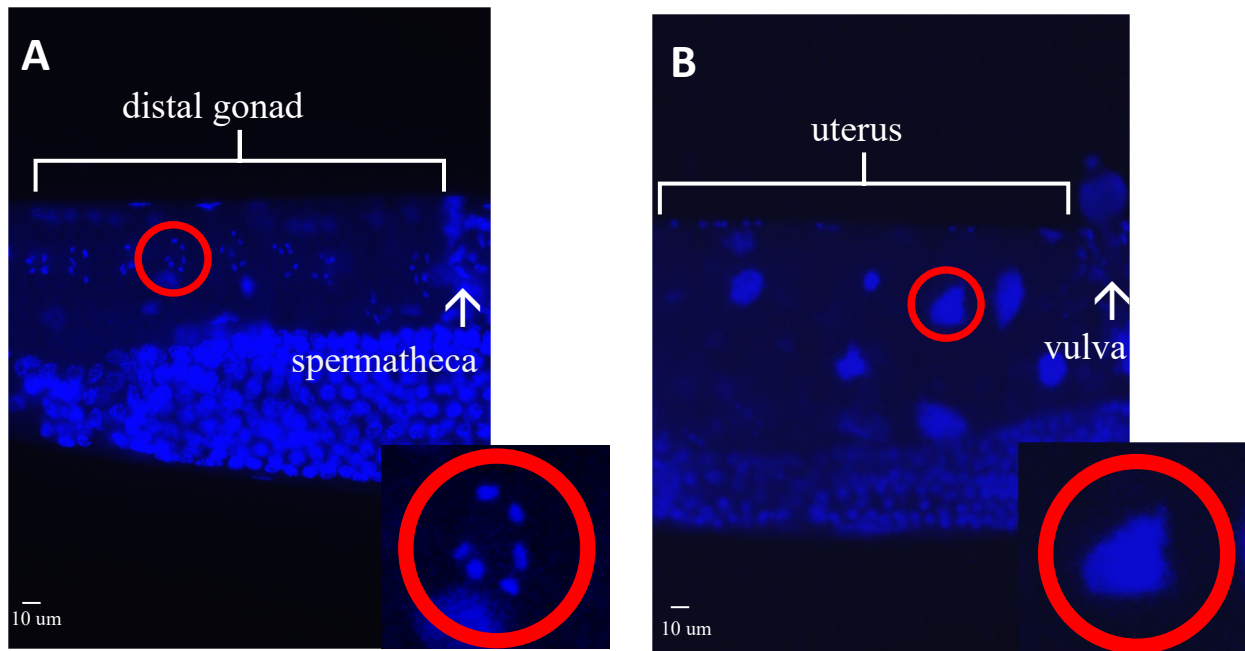


**Figure 2.** (A) nonEmo oocytes arrested in meiosis before entering the spermatheca. nonEmo oocyte in red circle enlarged in the corner. (B) Unfertilized Emo oocytes in the uterus. Emo oocyte in red circle enlarged in the corner.

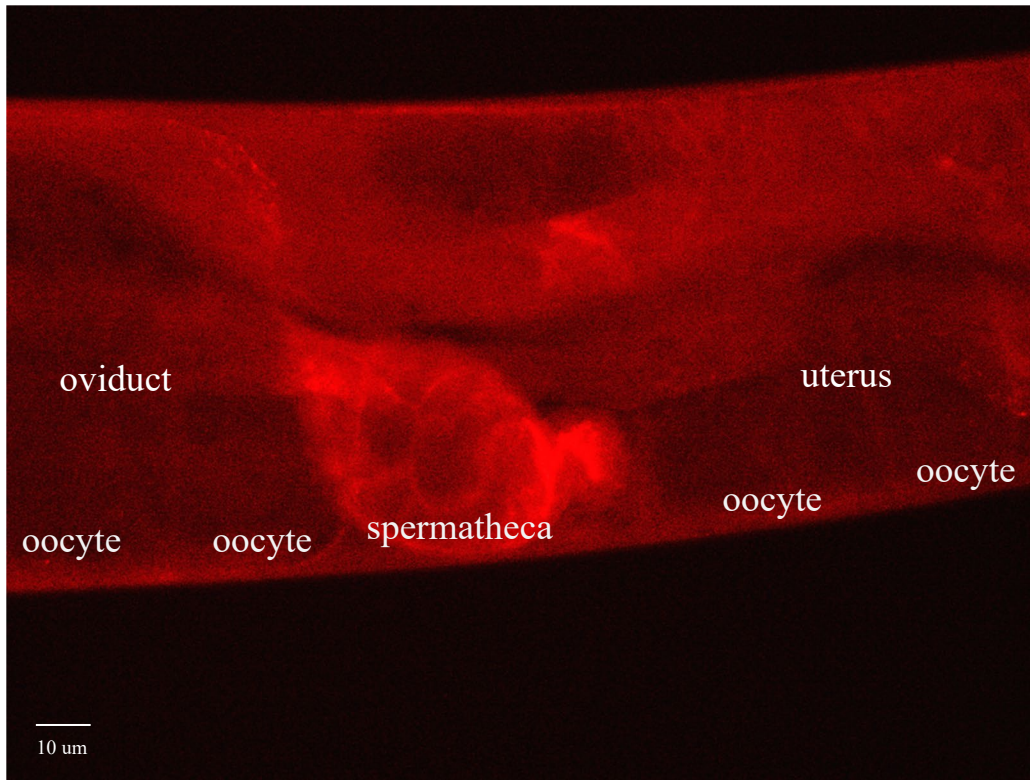


**Figure 3.** PEZO-1::mCherry is widely expressed throughout the worm including in the plasma membrane of oocytes and in the spermatheca. Picture taken by Elizabeth Gleason.

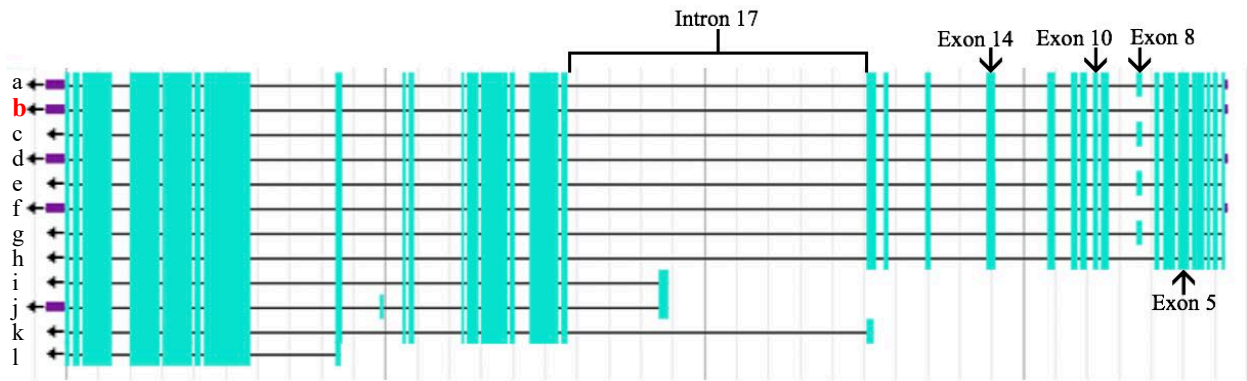


**Figure 4.** PEZO-1 isoforms in *Caenorhabditis elegans*. cDNA data for the 12 (a-l) isoforms are shown. Isoform b (bolded in red) represents the minimal form of PEZO-1 needed to cause the Emo phenotype. A stop opal nonsense mutation in exon 5 displayed the nonEmo phenotype. The Emo phenotype was still observed in the absence of exon 8, in either short and long forms of exon 10 and 14, or the presence or absence of the large intron 17. Blue regions are reverse transcripts, purple areas are 5' and 3' UTRs, and grey regions are noncoding transcripts. Modified screenshot from [www.wormbase.org](http://www.wormbase.org).

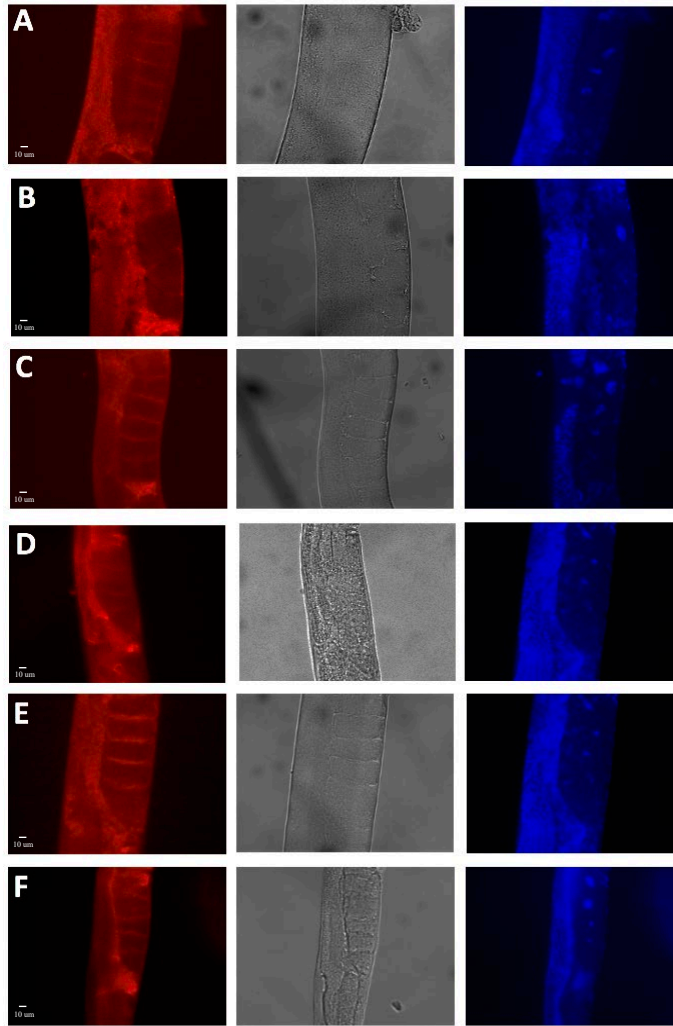


**Figure 5.** Micrographs of 25° raised worm strains expressing various *fer-1(b232) I*; *pezo-1::mCherry* IV isoforms. (A) SL1707 *fer-1(b232) I*; *pezo-1(ebIs33)::mCherry* IV. (B) SL1754 *fer-1(b232) I*; *pezo-1::mCherry (ebIs176)* IV (lacking exon 8 and including long exon 10). (C) SL1753 *fer-1(b232) I*; *pezo-1::mCherry (ebIs175)* I (lacking exon 8 and including short exon 10). (D) SL1765 *fer-1(b232) I*; *pezo-1::mCherry (ebIs62)* IV (lacking exon 8, including short exon 10, and lacking intron 17). (E) SL1776 *fer-1(b232) I*; *pezo-1::mCherry (ebIs71)* (lacking exon 8, including short exon 10, lacking intron 17, and including the long form of exon 14). (F) SL1777 *fer-1(b232) I*; *pezo-1::mCherry (ebIs72)* IV (lacking exon 8, including short exon 10, lacking intron 17, and including short exon 14).

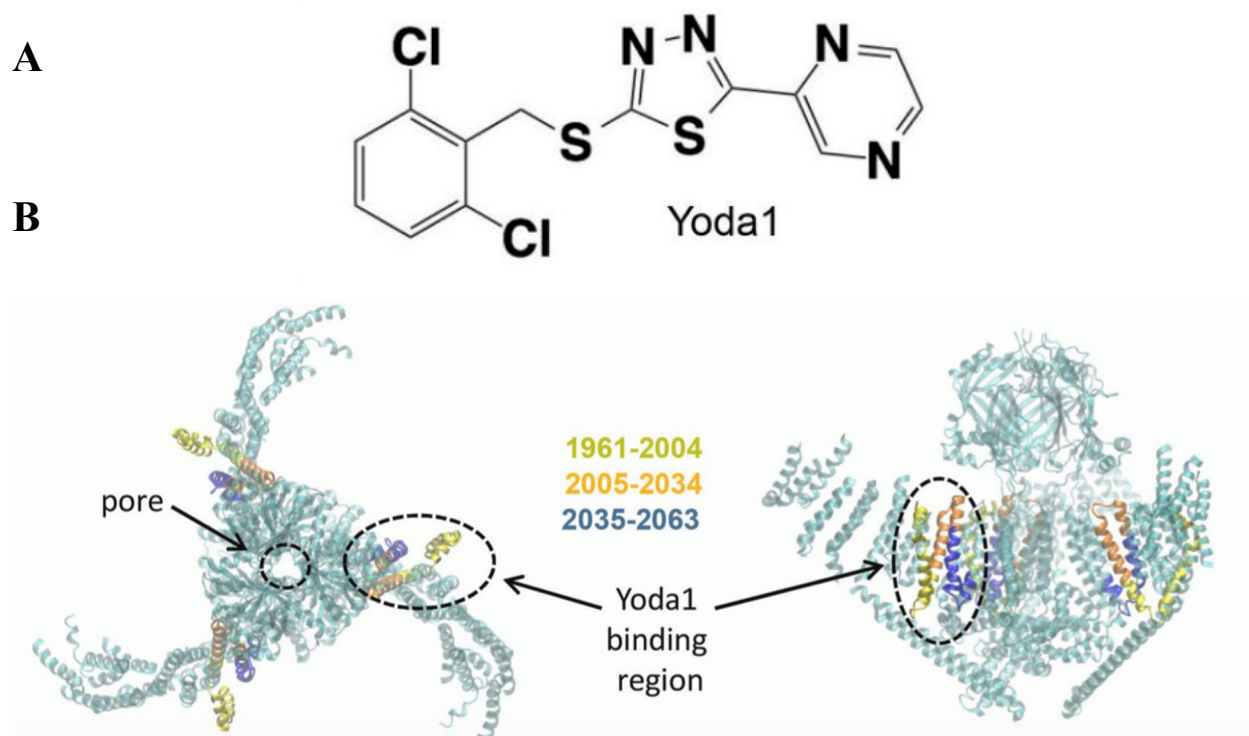


**Figure 6.** (A) Chemical structure of Yoda1. (B) Yoda1 allosteric binding region in mouse Piezo1 (from Lacroix, Botello-Smith, Luo, 2018).

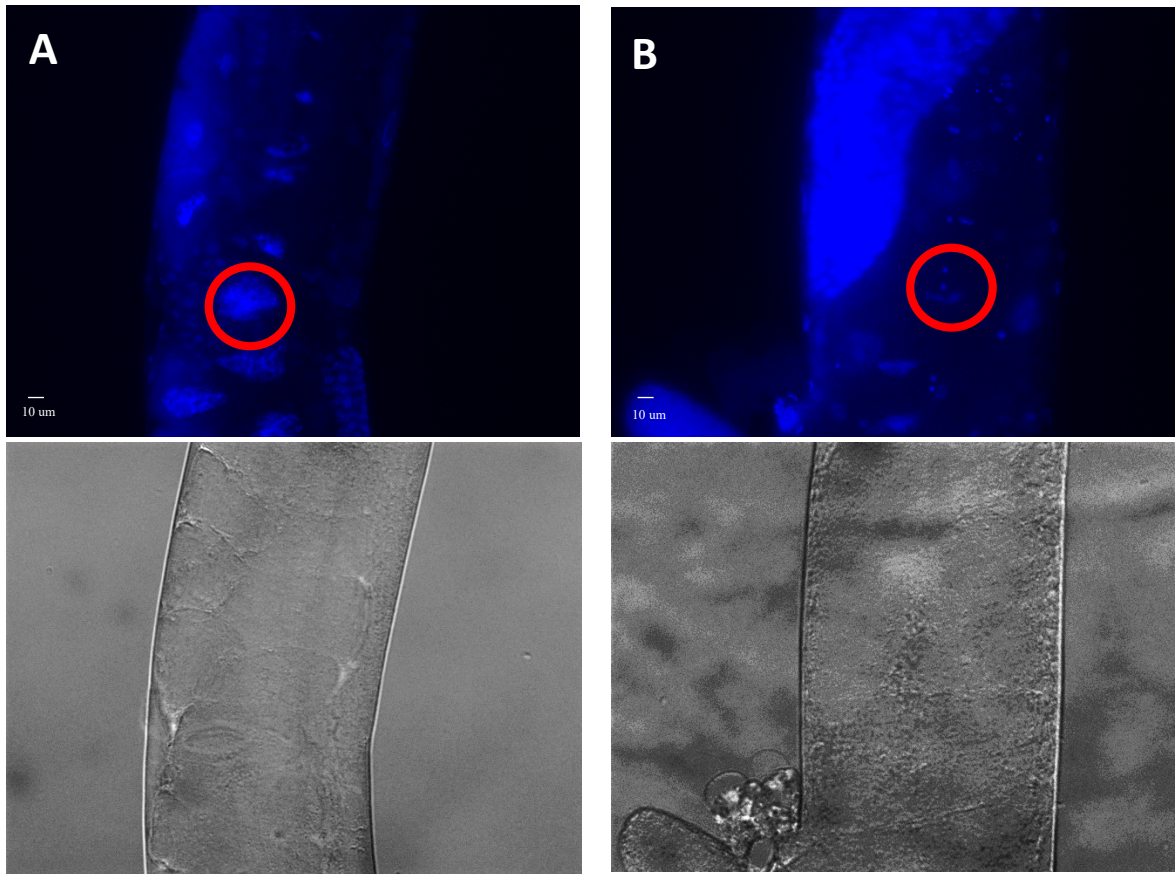


**Figure 7.** *fer-1(b232)* I worms exposed to 20 μM Yoda1. (A) A few control *fer-1(b232)* I worms on drug-free NGM agar have the Emo phenotype (Emo oocyte in red circle). (B) *fer-1(b232)* I worms raised on NGM agar plates with 20 μM Yoda1 (nonEmo oocyte in red circle).

	<b>Control, <i>fer-1(b232)</i> I worms on NGM</b>	<b><i>fer-1(b232)</i> I worms exposed to 20 <math>\mu</math>M Yoda1</b>
<b>% nonEmo</b>	4.5%	54.2%
<b>Total gonad arms</b>	22	24

**Table 1.** *fer-1(b232)* I worms exposed to Yoda1.

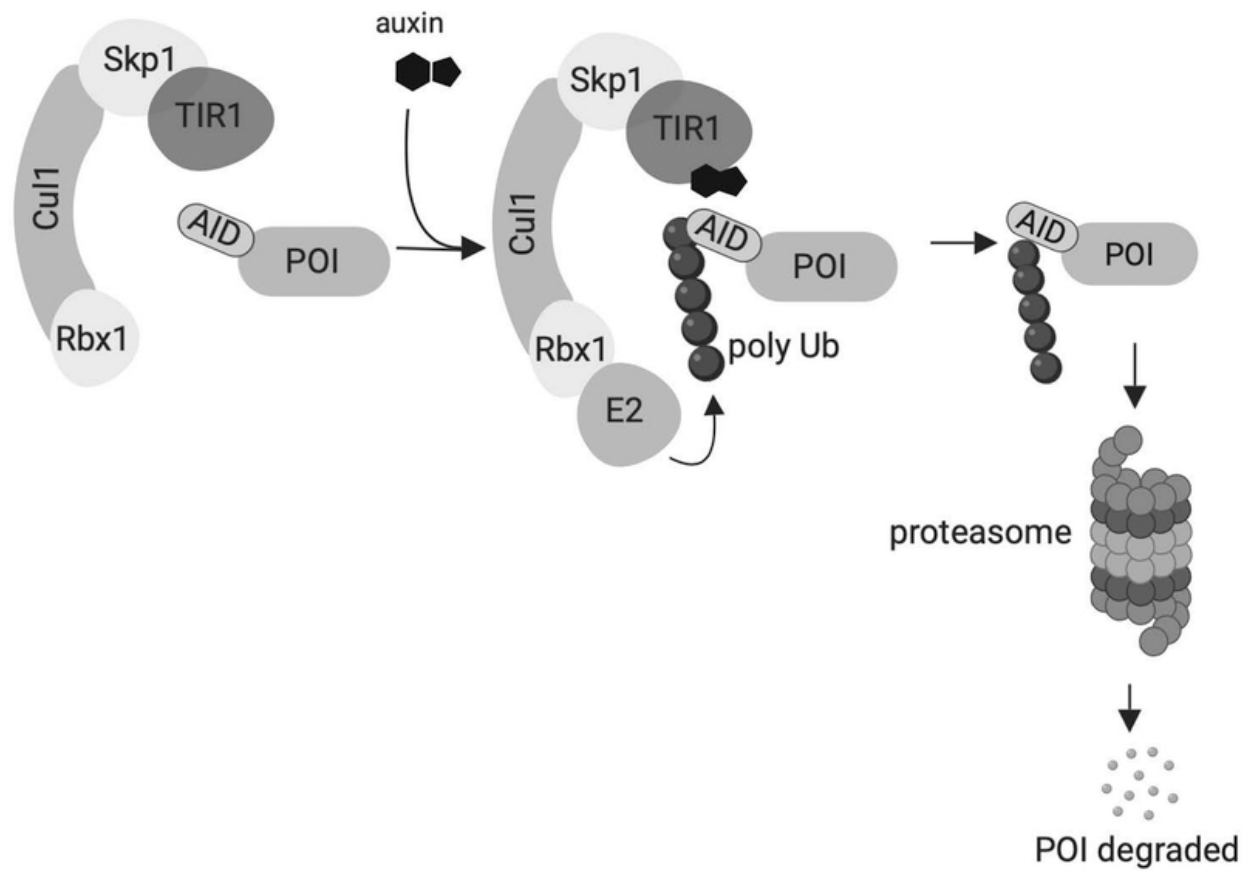


**Figure 8.** Auxin Inducible Degron System Mechanism (Shetty et al., 2019). TIR1 recognizes the degron sequence tagged onto the protein of interest (POI) in the presence of auxin.

	NGM TIR1 germline II; PEZO-1::mCh IV	Auxin TIR1 germline II; PEZO-1::mCh IV	NGM TIR1 somatic II; PEZO-1::mCh IV	Auxin TIR1 somatic II; PEZO-1::mCh IV	NGM TIR1 germline II; PEZO-1::GFP IV	Auxin TIR1 germline; PEZO-1::GFP IV	NGM TIR1 somatic II; PEZO-1::GFP IV	Auxin TIR1 somatic II; PEZO-1::GFP IV
% nonEmo	0%	65.4%	0%	37.5%	7.6%	88.9%	12.5%	83.3%
Total gonad arms	20	26	32	32	26	27	32	24

**Table 2.** *fer-1(b232) I; TIR1::mRuby II; degraon:: pezo-1::mCherry IV* and *fer-1(b232) I; TIR1::mRuby II; degraon:: pezo-1::GFP IV C. elegans* exposed to auxin.

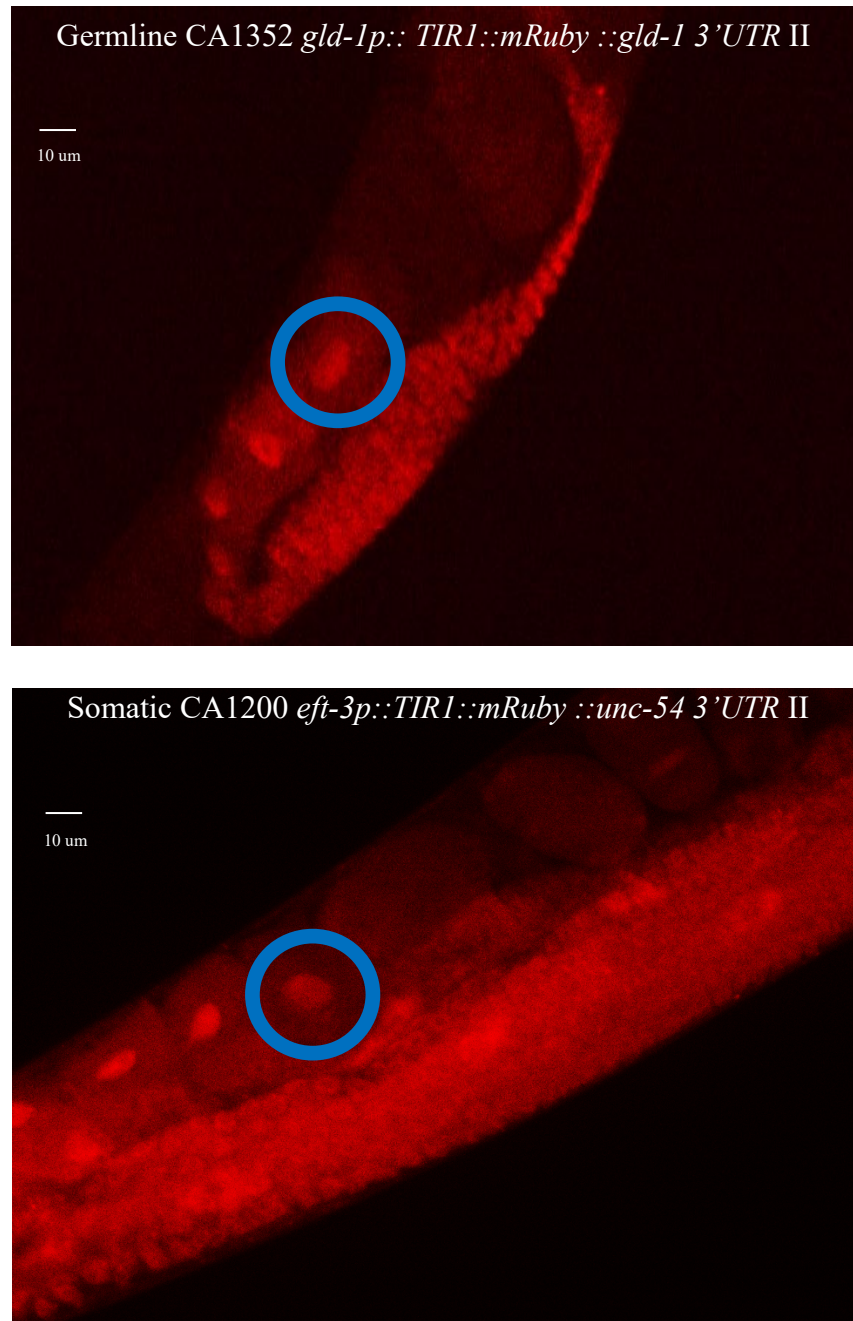


**Figure 9** Germline TIR1::mRuby line CA1352 *gld-1p:: TIR1::mRuby::gld-1 3'UTR II* and somatic TIR1::mRuby line CA1200 *eft-3p::TIR1::mRuby ::unc-54 3'UTR II* have red nuclei in the oocytes of the distal gonad (blue circles). (Will include scale bar).

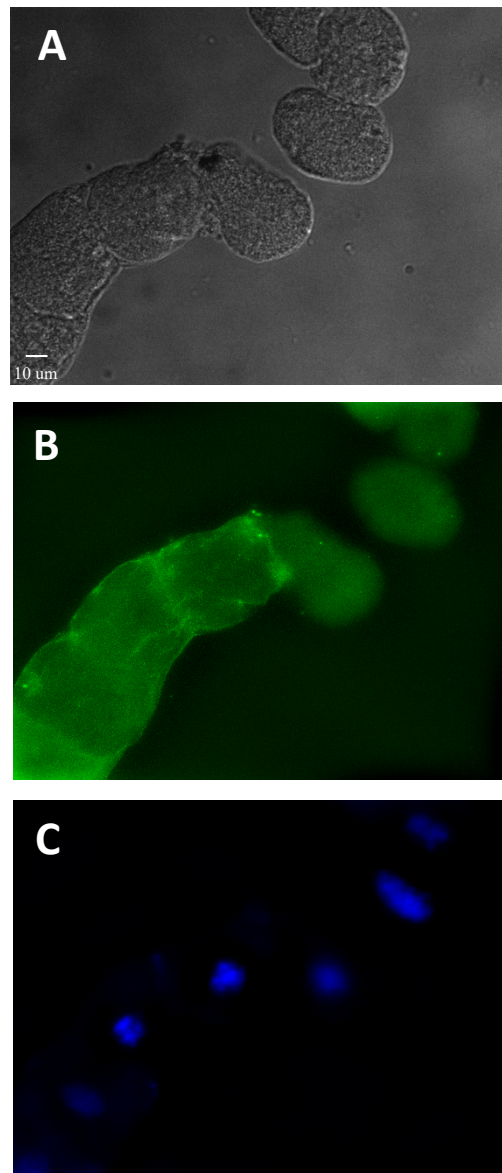
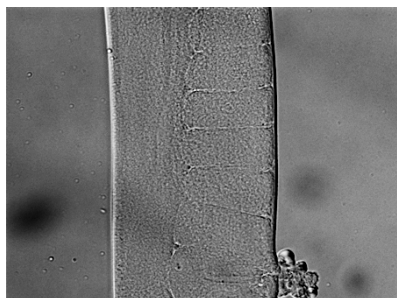
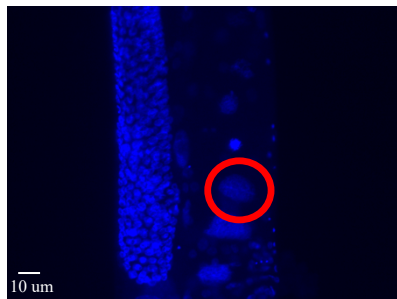
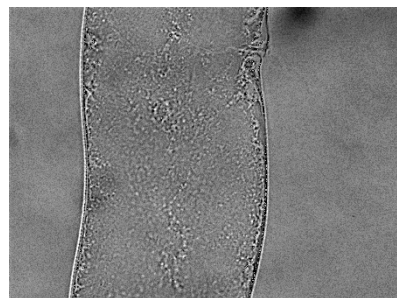
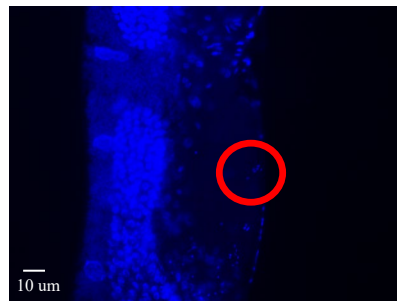


**Figure 10.** Immunofluorescence on *fer-1(b232)* I; *TIR1::mRuby* II; *degron::pezo-1::GFP* IV oocytes. (A) DIC. (B) FITC. (C) DAPI.

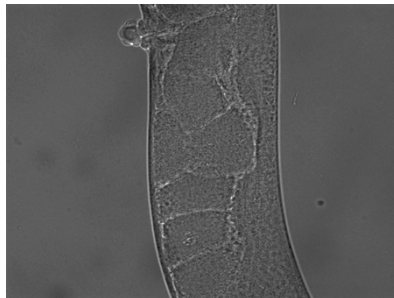
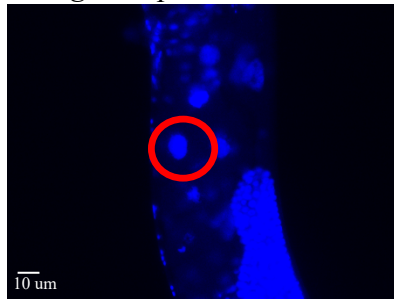
Control, *fer-1(b232)* I; *lucSi100*  
II (*hsp16.14::vhhGFP::zif-*  
*1::sl2::mCherry::his-11::tbb2*  
3'UTR), heat shocked for 30  
minutes



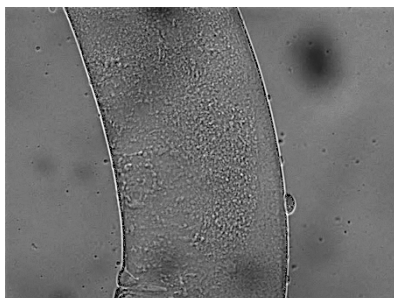
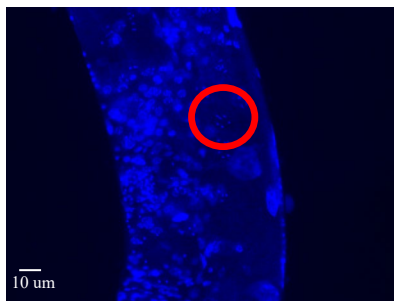
Heat shocked for 30  
minutes at 30°C, fixed  
after 2 hours



Control, *fer-1(b232)* I;  
*TIR1::mRuby* II;  
*degron::pezo-1::GFP* IV



Heat shocked for 30  
minutes at 30°C, fixed  
after 7 hours



Control, raised at  
25°C, no heat shock

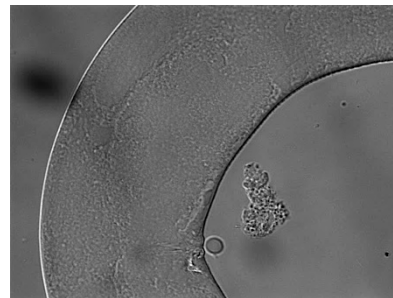
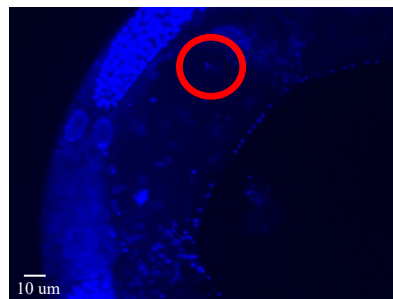


**Figure 11.** Heat Shock of *fer-1(b232)* I; *lucSi100* (*hsp16.41::vhhGFP::zif-*  
*1::SL2::mCherry::his-11::tbb2* 3'UTR)II; *degron::pezo-1::GFP* IV to Induce GFP Targeting  
Nanobody. (Will include scale bar).

	<b>Control, line with GFP but no heat shock system, heat shocked for 30 minutes</b>	<b>Control, line with heat shock system but no GFP, heat shocked for 30 minutes</b>	<b>Control, with heat shock system, no heat shock, raised at 25°C</b>	<b>Heat shocked for 30 minutes at 30°C, fixed after 2 hours</b>	<b>Heat shocked for 30 minutes at 30°C, fixed after 7 hours</b>
<b>Percent nonEmo</b>	7.6%	12.5%	46%	75%	93%
<b>Total gonad arms screened</b>	26	24	37	16	14

**Table 3.** Heat Shock of *fer-1(b232)* I; *lucSi100* (*hsp16.41::vhhGFP::zif-1::SL2::mCherry::his-11::tbb2 3'UTR*)II; *degron::pezo-1::GFP* IV to Induce GFP Targeting Nanobody.

## References

- Argon, Y., and Ward, S. (1980). *Caenorhabditis elegans* fertilization-defective mutants with abnormal sperm. *Genetics* 96, 413–433.
- Bai, X., Bouffard, J., Lord, A., Brugman, K., Sternberg, P.W., Cram, E.J., and Golden, A. (2020). *Caenorhabditis elegans* piezo channel coordinates multiple reproductive tissues to govern ovulation. *Elife* 9, 1–35.
- Charest, J., Daniele, T., Wang, J., Bykov, A., Mandlbauer, A., Asparuhova, M., Röhsner, J., Gutiérrez-Pérez, P., and Cochella, L. (2020). Combinatorial Action of Temporally Segregated Transcription Factors. *Dev. Cell* 55, 483–499.e7.
- del Marmol, J.I., Touhara, K.K., Croft, G., and MacKinnon, R. (2018). Piezo1 forms a slowly-inactivating mechanosensory channel in mouse embryonic stem cells. *Elife* 7, 1–18.
- Ge, J., Li, W., Zhao, Q., Li, N., Chen, M., Zhi, P., Li, R., Gao, N., Xiao, B., and Yang, M. (2015). Architecture of the mammalian mechanosensitive Piezo1 channel. *Nature* 527, 64–69.
- Greenstein, D. (2005). Control of oocyte meiotic maturation and fertilization. *WormBook* 1–12.
- Guerin, S., Tofail, S.A.M., and Thompson, D. (2019). Organic piezoelectric materials: milestones and potential. *NPG Asia Mater.* 11, 2021.
- Harris, T.W., Arnaboldi, V., Cain, S., Chan, J., Chen, W.J., Cho, J., Davis, P., Gao, S., Grove, C.A., Kishore, R., et al. (2020). WormBase: A modern Model Organism Information Resource. *Nucleic Acids Res.* 48, D762–D767.
- He, L., Si, G., Huang, J., Samuel, A.D.T., and Perrimon, N. (2018). Mechanical regulation of stem-cell differentiation by the stretch-activated Piezo channel. *Nature* 555, 103–106.
- Hiatt, S.M., Duren, H.M., Shyu, Y.J., Ellis, R.E., Hisamoto, N., Matsumoto, K., Kariya, K.I., Kerppola, T.K., and Hu, C.D. (2009). *Caenorhabditis elegans* FOS-1 and JUN-1 regulate plc-1 expression in the spermatheca to control ovulation. *Mol. Biol. Cell* 20, 3888–3895.
- Koptsik, V.A., and Rez, I.S. (1981). Pierre Curie's Works in the Field of Crystal Physics (On the One-Hundredth Anniversary of the Discovery of the Piezoelectric Effect). *Sov. Phys. - Uspekhi* 24, 426–428.
- Kovacevic, I., Orozco, J.M., and Cram, E.J. (2013). Filamin and Phospholipase C-ε Are Required for Calcium Signaling in the *Caenorhabditis elegans* Spermatheca. *PLoS Genet.* 9.
- Lacroix, J.J., Botello-Smith, W.M., and Luo, Y. (2018). Probing the gating mechanism of the mechanosensitive channel Piezo1 with the small molecule Yoda. *Nat. Commun.* 9.

- L'Hernault, S.W. (2009). The genetics and cell biology of spermatogenesis in the nematode *C. elegans*. *Mol. Cell. Endocrinol.* *306*, 59–65.
- Li, J., Hou, B., Tumova, S., Muraki, K., Bruns, A., Ludlow, M.J., Sedo, A., Hyman, A.J., McKeown, L., Young, R.S., et al. (2014). Piezo1 integration of vascular architecture with physiological force. *Nature* *515*, 279–282.
- McCarter, J., Bartlett, B., Dang, T., and Schedl, T. (1997). Soma-germ cell interactions in *Caenorhabditis elegans*: Multiple events of hermaphrodite germline development require the somatic sheath and spermathecal lineages. *Dev. Biol.* *181*, 121–143
- Merritt, C., Rasoloson, D., Ko, D., and Seydoux, G. (2008). 3' UTRs Are the Primary Regulators of Gene Expression in the *C. elegans* Germline. *Curr. Biol.* *18*, 1476–1482.
- Nigon, V.M., and Félix, M. (2017). History of research on *C. elegans* and other free-living nematodes as model organisms. *WormBook* 1–84.
- Nishimura, H., and L'Hernault, S.W. (2010). Spermatogenesis-defective (spe) mutants of the nematode *Caenorhabditis elegans* provide clues to solve the puzzle of male germline functions during reproduction. *Dev. Dyn.* *239*, 1502–1514.
- Nonomura, K., Lukacs, V., Sweet, D.T., Goddard, L.M., Kanie, A., Whitwam, T., Ranade, S.S., Fujimori, T., Kahn, M.L., and Patapoutian, A. (2018). Mechanically activated ion channel PIEZO1 is required for lymphatic valve formation. *Proc. Natl. Acad. Sci. U. S. A.* *115*, 12817–12822.
- Nonomura, K., Woo, S.H., Chang, R.B., Gillich, A., Qiu, Z., Francisco, A.G., Ranade, S.S., Liberles, S.D., and Patapoutian, A. (2017). Piezo2 senses airway stretch and mediates lung inflation-induced apnoea. *Nature* *541*, 176–181.
- Syeda, R., Xu, J., Dubin, A.E., Coste, B., Mathur, J., Huynh, T., Matzen, J., Lao, J., Tully, D.C., Engels, I.H., et al. (2015). Chemical activation of the mechanotransduction channel Piezo1. *Elife* *4*, 1–11.
- Shetty, A., Reim, N.I., and Winston, F. (2019). Auxin-Inducible Degron System for Depletion of Proteins in *Saccharomyces cerevisiae*. *Curr. Protoc. Mol. Biol.* *128*, e104.
- Spike, C., Meyer, N., Racen, E., Orsborn, A., Kirchner, J., Kuznicki, K., Yee, C., Bennett, K., and Strome, S. (2008). Genetic analysis of the *Caenorhabditis elegans* GLH family of P-granule proteins. *Genetics* *178*, 1973–1987.
- Teale, W.D., Paponov, I.A., and Palme, K. (2006). Auxin in action: Signalling, transport and the control of plant growth and development. *Nat. Rev. Mol. Cell Biol.* *7*, 847–859.

Tenenhaus, C., Subramaniam, K., Dunn, M.A., and Seydoux, G. (2001). PIE-1 is a bifunctional protein that regulates maternal and zygotic gene expression in the embryonic germ line of *Caenorhabditis elegans*. *Genes Dev.* *15*, 1031–1040.

Thompson, O., Edgley, M., Strasbourger, P., Flibotte, S., Ewing, B., Adair, R., Au, V., Chaudhry, I., Fernando, L., Hutter, H., et al. (2013). The million mutation project: A new approach to genetics in *Caenorhabditis elegans*. *Genome Res.* *23*, 1749–1762.

Woo, S.H., Lukacs, V., De Nooij, J.C., Zaytseva, D., Criddle, C.R., Francisco, A., Jessell, T.M., Wilkinson, K.A., and Patapoutian, A. (2015). Piezo2 is the principal mechanotransduction channel for proprioception. *Nat. Neurosci.* *18*, 1756–1762.

Woo, S.H., Ranade, S., Weyer, A.D., Dubin, A.E., Baba, Y., Qiu, Z., Petrus, M., Miyamoto, T., Reddy, K., Lumpkin, E.A., et al. (2014). Piezo2 is required for Merkel-cell mechanotransduction. *Nature* *509*, 622–626.

Xiong, H., Pears, C., and Woollard, A. (2017). An enhanced *C. elegans* based platform for toxicity assessment. *Sci. Rep.* *7*, 1–11.

Zhang, L., Ward, J.D., Cheng, Z., and Dernburg, A.F. (2015). The auxin-inducible degradation (AID) system enables versatile conditional protein depletion in *C. elegans*. *Dev.* *142*, 4374–4384.